

## COMMUNICATION

[View Article Online](#)  
[View Journal](#) | [View Issue](#)

Cite this: *Polym. Chem.*, 2023, **14**, 2022

Received 17th March 2023,

Accepted 16th April 2023

DOI: 10.1039/d3py00287j

rsc.li/polymers

## Responsive tertiary amine methacrylate block copolymers: uncovering temperature-induced shape-shifting behaviour†

Zahn Stanvliet,<sup>a</sup> Yiyi Deng,<sup>b</sup> Dietmar Appelhans,<sup>b</sup> Silvia Moreno,<sup>b</sup> Susanne Boye,<sup>b</sup> Jens Gaitzsch<sup>\*b</sup> and Alben Lederer<sup>†\*</sup>

**Responsive polymeric nanoparticles are an exciting field of study, yet little is known about the temperature sensitivity of those based on tertiary amine methacrylate block copolymers. This study aims to address this gap by exploiting the properties of dual-responsive amphiphilic block copolymers. Here, we investigate the fabrication of self-assembled polymeric nanoparticles using block copolymers containing tertiary amine methacrylate building blocks and their ability to undergo a reversible morphological transformation upon changes in pH and temperature. Our findings demonstrate the ability to change the morphology after adjusting temperature, lock their various intermediate self-assembly structures through cross-linking, and a combination of analytical tools to validate morphology transition, opening up new options for responsive nanocarriers.**

Polymers that exhibit reversible or irreversible changes in their physical properties and/or chemical structure in response to stimuli have been extensively investigated.<sup>1–5</sup> Tertiary amine polymers are a special class as they respond to various stimuli which are relevant to the biological environment. Such interesting properties have caused them to be useful in a variety of fields ranging from drug or gene delivery, and imaging, to diagnostics and more.<sup>6–8</sup> Tertiary amine methacrylate polymers typically display pH-responsive characteristics as a result of the reversible protonation and deprotonation of the tertiary amines. They may also have temperature-responsive characteristics, allowing them to alter their solubility when heated or cooled. Both poly(*N,N*-dimethylaminoethyl methacrylate) (PDMA) and poly(*N,N*-diethylaminoethyl methacrylate) (PDEA) exhibit a so-called lower critical solution temperature (LCST) behaviour, meaning that these polymers phase-separate from

water at elevated temperatures, while the aqueous solutions are stable below the LCST.<sup>7</sup> While responsivity studies of nanoparticles derived from tertiary-amine methacrylate block copolymers mainly focus on their well-known pH-responsivity,<sup>9</sup> studies on their temperature-responsive behaviour remain largely unexplored as it was only looked into for the isopropyl-derivative.<sup>10,11</sup> In this study, we aimed to produce temperature-sensitive nanoparticles fabricated from tertiary amine-based block copolymers. They were designed to undergo a reversible temperature-dependent morphological transition described by Thavanesan *et al.*<sup>7</sup> An additional cross-linking was then added to suppress this transition and to enable precise analysis of these structures (Fig. 1). Together with a pH switch at lower temperatures, this study was designed to exploit the dual-responsiveness of PDEA and PDMA in a single self-assembly system.

To examine this behaviour, an amphiphilic block copolymer (BCP) with the following components was used. The hydrophilic block consisted of biocompatible poly(ethylene glycol) (PEG), while the hydrophobic block was a statistical combination of three components, including the pH and temperature sensitive PDEA and PDMA together with the photo cross-linker poly(dimethyl maleic imido butyl methacrylate) (PDMI). The resulting PEG<sub>45</sub>-*b*-(PDEA<sub>49</sub>-*s*-PDMA<sub>27</sub>-*s*-PDMI<sub>24</sub>) (Fig. 1), previously reported along with similar compositions by Gumz *et al.*, has been used for nanoparticle formation and labelled as PEG-PDEA-PDMA-PDMI.<sup>12,13</sup> The synthesis and characterization of the BCP is described in the ESI.† The BCP self-assembles into polymeric vesicles (polymerosomes) and can be cross-linked by UV radiation to enhance the stability of the membrane and cause a reversible swelling upon a pH switch. Self-assembly was induced *via* the pH-switch method previously reported and described in the ESI.†<sup>10,12,14</sup> The pH switch point is defined by the alkyl chain conjugated to the tertiary amine, which influences the p*K*<sub>a</sub> of the polymers. PDMAEMA and PDEAEMA homopolymers have p*K*<sub>a</sub> values of 7.0–7.5 and 7.2–7.4, respectively.<sup>6</sup>

The self-assembly of the BCP produced polymerosomes with an average hydrodynamic diameter of 40 nm was followed

<sup>a</sup>Stellenbosch University, Department of Chemistry and Polymer Science, Private Bag X1, Matieland, 7602, South Africa. E-mail: alederer@sun.ac.za, lederer@ipfdd.de

<sup>b</sup>Leibniz-Institut für Polymerforschung Dresden e.V., Hohe Str. 6, 01069 Dresden, Germany. E-mail: gaitzsch@ipfdd.de

† Electronic supplementary information (ESI) available. See DOI: <https://doi.org/10.1039/d3py00287j>

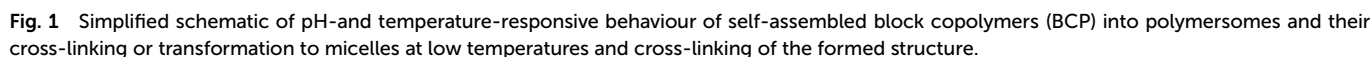


Figure 1 consists of three panels. Panel (A) is a transmission electron micrograph (TEM) showing several spherical polymeric virus-like particles (VLPs) with a 200 nm scale bar. An inset shows a schematic of a VLP with a green core, orange shell, and green spikes. Panel (B) is a DLS volume distribution plot showing the effect of heating. The x-axis is 'Hydrodynamic diameter (nm)' on a log scale from 1 to 100. The y-axis is 'Volume (%)' from 0 to 16. Two curves are shown: a green curve for 20 °C and a red curve for 40 °C. Both curves show a single peak at approximately 30 nm. Panel (C) is a DLS volume distribution plot showing the effect of cooling. The x-axis is 'Hydrodynamic diameter (nm)' on a log scale from 1 to 100. The y-axis is 'Volume (%)' from 0 to 20. Two curves are shown: a green curve for 20 °C and a blue curve for 3 °C (48 h). The green curve has a peak at approximately 30 nm, and the blue curve has a peak at approximately 20 nm.

**Fig. 2** (A) Cryo-TEM image of cross-linked polymersomes confirming broad size distributions as observed with DLS. (B) Volume size distribution of non-cross-linked polymersomes at 20 °C and 40 °C (pH 9) determined by DLS, displaying no responsivity toward elevated temperatures. (C) Volume size distribution of non-cross-linked polymersomes at 20 °C and 3 °C, displaying responsivity toward low temperatures by undergoing a change in size toward smaller sizes.

assembly process. Free polymer chains remain encapsulated in the developing polymersome or polymersome membrane during self-assembly (high pH) and are released after swelling

(low pH). The observed molar mass ( $M_w$ ) supports this explanation. Polymersomes in the swollen state have a slightly lower  $M_w$  than those in the shrunken state, also suggesting that material has been lost. Swollen polymersomes also have a lower apparent density than shrunken polymersomes (Fig. SI14D†). Two aspects are looked at as an explanation: (I) an increased radius of gyration ( $R_g$ ) owing to swelling and (II) a lower  $M_w$  due to a loss of material or uncross-linked BCPs that “leak”. The polymersome conformation plot in Fig. SI14C† at pH 8.5 and pH 5, indicate two different species in the low and high  $M_w$  region. For pH 8.5, a more compact spherical conformation is observed in the low  $M_w$  region (lower slope), whereas less compact polymersomes are seen in the high  $M_w$  region ( $\nu = 0.48$ , close to 0.33 for a hard sphere conformation).<sup>19,20</sup> The ratio  $R_g/R_h$  describes the shape of particles and is called the shape factor.  $R_g/R_h$  is close to 1, in the molar mass region for the main polymersome fraction, which is common for hollow spheres (Table SI3†).<sup>16,18</sup>

Slight changes of the membrane are observed at the different pH conditions. At pH 5, the low  $M_w$  region has a slightly greater slope than the slope at higher  $M_w$  which shows that polymersomes are keeping a spherical conformation after swelling with minor difference in the scaling parameter ( $\nu = 0.43$  at pH 5 respectively) as shown in Fig. SI14C.†

The temperature-responsive behaviour of cross-linked and uncross-linked polymersomes was investigated through DLS by varying the solution temperature between 20 °C and 40 °C while maintaining a constant pH = 9. In all cases, no changes were observed when the temperature was increased (Fig. 2B). Control experiments with PEG-PDEA-PDMI (Fig. SI9†) and PEG-PDEA (Fig. SI11†) also showed no size response upon heating in the same range. The investigation was continued at low temperatures, varying the temperature between 20 °C and 5 °C while maintaining a constant pH. For uncross-linked polymersomes, the appearance of an additional signal is observed giving the indication that there exist additional smaller structures when the temperature decreases (Fig. SI8†). This particular sample was kept at 3 °C for 48 h leading to a change in the size distribution, which revealed that the polymersomes underwent a significant size decrease going from a hydrodynamic diameter of 40 nm to 17 nm (Fig. 2C).

This temperature-dependent transition is proposed to be a morphological transition. This size change was due to PDMA as cooling PEG-PDEA-PDMI lead to no change in size (Fig. SI10†). The shape-shifting behavior observed for some aqueous dispersions of temperature-responsive diblock copolymer nanostructures is the consequence of a subtle change in the relative degree of hydration of the hydrophobic block. Surface plasticization of the insoluble structure-directing block causes a slight adjustment in the packing parameter, resulting in a morphological transition from small polymersomes to smaller structures, possibly micelles.<sup>21</sup> Cross-linking prevented this transition as no changes were observed, again demonstrating the stability that can be introduced by cross-linking (Fig. SI7†). To examine the unknown smaller structure, a solution of uncross-linked polymersome was stored under the

same conditions that caused the size decrease. In order to keep the formed structure, the solution was then immediately cross-linked and subjected to a temperature study. Cross-linking succeeded to prevent the structures from reverting to their initial size, again stabilizing the self-assembled structure at low temperature present before cross-linking. This allowed for the structures to be analyzed by cryo-TEM (Fig. 3A). The polymersome structure was not visible anymore but spherical morphologies, most likely micelles or polymer agglomerates, were recognized. It should be mentioned that some formations had uneven edges, while others strayed from a spherical shape. Nonetheless, it served as proof that a morphological transition occurred.

The unknown morphology of PEG-PDEA-PDMA-PDMI was then analyzed by AF4 (Fig. 4). Interestingly, the size of these

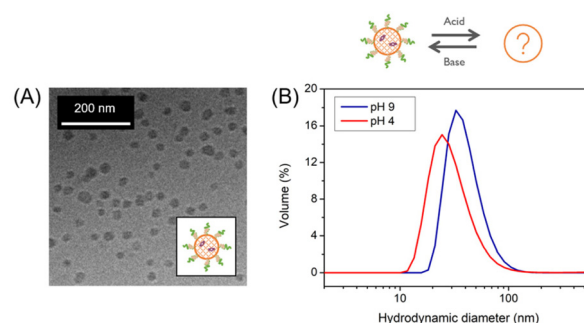


**Fig. 3** (A) Cryo-TEM images of the cross-linked structure, revealing spherical morphologies. Confirms that polymersomes underwent a morphological transition. (B) Volume size distribution of cross-linked micelle structure showing a decrease in size upon acidification.

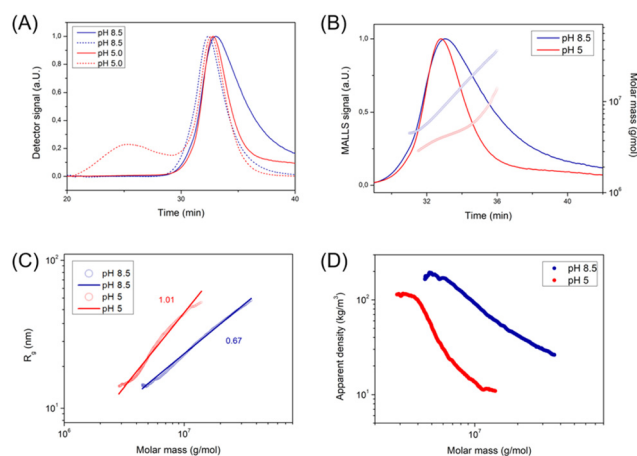


**Fig. 4** pH-dependent structural parameters determined by AF4 of cross-linked micelle structure at basic (pH 8.5, blue) and acidic (pH 5, red) conditions. (A) AF4 fractograms of micelle structure displaying static light scattering (solid) and refractive index detector signals (dashed). (B) Static light scattering signal and molar mass ( $M_w$ ) distribution versus elution time. (C) Conformation plot,  $M_w$  vs. radius ( $R_g$ ). (D) Apparent density is calculated according to  $M_w$  and  $R_g$ , assuming a spherical shape. Conditions:  $c_{BCP} = 1.0 \text{ mg mL}^{-1}$ , 10 mM NaCl.



structures shrunk as the environment became more acidic as demonstrated in the DLS plots (Fig. 3B). At both pH conditions,  $R_g/R_h$  is between that of a hard and a hollow sphere ( $0.7 < R_g/R_h < 1.0$ ) indicating a compact shape (Table SI4†).<sup>16,22</sup> Yet, the scaling parameter  $\nu$  is rather large (0.67–1.01) corresponding to a conformation between that of a random coil and a stiff, rod-like conformation (Fig. 4C).<sup>23</sup> The shape is dependent on the solution pH as can be seen by the difference between the scaling parameters. It is still unclear what leads to the high scaling parameter under these conditions or why the shape is affected by the solution pH. This contrary behavior to polymersomes 20 °C indicated that the micelles did not swell upon acidification, but that the loss of material became the dominating factor. This hypothesis is supported by the development of a second population under acidic conditions, comparable to that of polymersomes. This was consistent with the observed non-assembled BCP, as discussed for the swelling of the polymersomes. Given that these structures do not swell (neither a change toward longer elution times in AF4 nor a change toward larger diameters in DLS under acidic conditions was observed), it seems unlikely that free BCP chains become trapped in the core of the developing structure and are released when exposed to acidic conditions. However, a loss of material at acidic conditions is supported as indicated by the decreased apparent density and decreased  $M_w$ . One possibility is that free BCPs adhere to the surface and are released with acidification. This phenomenon is likely to explain both, the less homogeneous shape and uneven surface, as well as why the hydrodynamic size decreases at acidic conditions.

## Conclusions

In summary, PEG-PDEA-PDMA-PDMI nanoparticles exhibit a pronounced temperature-dependent shape-shifting behavior at low temperatures. The pH-switch approach was used to fabricate these nanoparticles in water. These could be cross-linked after which they undergo reversible swelling and shrinking upon adjusting the solution pH. When adjusting the solution temperature, these nanoparticles undergo a reversible morphological shift from membrane (polymersomes) to micelles. Cross-linking enabled the suppression of this transition and in-depth characterization of the different shapes using multi-detection AF4, DLS and cryo-TEM.

## Conflicts of interest

There are no conflicts to declare.

## Acknowledgements

We thank financial support by the Postgraduate Scholarship Program of Stellenbosch University, and the assistance of Dr Petr Formanek (Cryo-TEM), Mr Andreas Schurig (BCP syn-

thesis), Ms Alissa Seifert (SEC analysis) and Ms Franzisca Kucharczyk (self-assembly) from the Leibniz-Institut für Polymerforschung Dresden e.V.

## References

- 1 S. S. Das, P. Bharadwaj, M. Bilal, M. Barani, A. Rahdar, P. Taboada, S. Bungau and G. Z. Kyzas, *Polymers*, 2020, **12**(6), 1397.
- 2 Y. J. Kim and Y. T. Matsunaga, *J. Mater. Chem. B*, 2017, **5**, 4307–4321.
- 3 H. Che and J. C. M. Van Hest, *J. Mater. Chem. B*, 2016, **4**, 4632–4647.
- 4 Q. Zhou, L. Zhang, T. H. Yang and H. Wu, *Int. J. Nanomed.*, 2018, **13**, 2921–2942.
- 5 C. Yao, X. Wang, G. Liu, J. Hu and S. Liu, *Macromolecules*, 2016, **49**, 8282–8295.
- 6 J. Hu, G. Zhang, Z. Ge and S. Liu, *Prog. Polym. Sci.*, 2014, **39**, 1096–1143.
- 7 T. Thavanesan, C. Herbert and F. A. Plamper, *Langmuir*, 2014, **30**, 5609–5619.
- 8 B. Pang, Y. Yu and W. Zhang, *Macromol. Rapid Commun.*, 2021, **42**, 1–17.
- 9 J. Gaitzsch, X. Huang and B. Voit, *Chem. Rev.*, 2016, **116**, 1053–1093.
- 10 R. T. Pearson, N. J. Warren, A. L. Lewis, S. P. Armes and G. Battaglia, *Macromolecules*, 2013, **46**, 1400–1407.
- 11 C. Contini, R. Pearson, L. Wang, L. Messenger, J. Gaitzsch, L. Rizzello, L. Ruiz-Perez and G. Battaglia, *iScience*, 2018, **7**, 132–144.
- 12 H. Gumz, T. H. Lai, B. Voit and D. Appelhans, *Polym. Chem.*, 2017, **8**, 2904–2908.
- 13 M. Palinske, U. L. Muza, S. Moreno, D. Appelhans, S. Boye, R. Schweins and A. Lederer, *Macromol. Chem. Phys.*, 2023, **224**(1), 2200300.
- 14 L. Messenger, J. Gaitzsch, L. Chierico and G. Battaglia, *Curr. Opin. Pharmacol.*, 2014, **18**, 104–111.
- 15 S. Moreno, B. Voit and J. Gaitzsch, *Colloid Polym. Sci.*, 2021, **299**, 309–324.
- 16 S. Moreno, P. Sharan, J. Engelke, H. Gumz, S. Boye, U. Oertel, P. Wang, S. Banerjee, R. Klajn, B. Voit, A. Lederer and D. Appelhans, *Small*, 2020, **16**, 1–11.
- 17 S. Moreno, S. Boye, H. G. Al Ajeilat, S. Michen, S. Tietze, B. Voit, A. Lederer, A. Temme and D. Appelhans, *Macromol. Biosci.*, 2021, **21**, 1–12.
- 18 S. Moreno, S. Boye, A. Lederer, A. Falanga, S. Galdiero, S. Lecommandoux, B. Voit and D. Appelhans, *Biomacromolecules*, 2020, **21**, 5162–5172.
- 19 H. Gumz, S. Boye, B. Iyisan, V. Krönert, P. Formanek, B. Voit, A. Lederer and D. Appelhans, *Adv. Sci.*, 2019, **6**(7), 1970037.



- 20 E. Geervliet, S. Moreno, L. Baiamonte, R. Booiijink, S. Boye, P. Wang, B. Voit, A. Lederer, D. Appelhans and R. Bansal, *J. Controlled Release*, 2021, **332**, 594–607.
- 21 O. J. Deane, J. Jennings and S. P. Armes, *Chem. Sci.*, 2021, **12**, 13719–13729.
- 22 M. Glantz, A. Håkansson, H. Lindmark Månsson, M. Paulsson and L. Nilsson, *Langmuir*, 2010, **26**, 12585–12591.
- 23 S. E. Harding, A. S. Abdelhameed and G. A. Morris, *Polym. Int.*, 2011, **60**, 2–8.

